# RECONSTRUCTION OF THE GLOBAL NON-LINEAR FORCE-FREE SOLAR CORONAL MAGNETIC FIELD

Contopoulos, Kalapotharakos, Georgoulis 2011, Solar Physics

Ioannis Contopoulos

RCAAM Academy of Athens

# OUTLINE

- The Solar Corona
- Numerical methods
- Force-Free Electrodynamics
- Results
- Prospects for the future

# THE SOLAR CORONA

$$\mathbf{J} \times \mathbf{B} = 0$$

- The solar `atmosphere'
- Gas temperatures: $10^4$-$10^7$ °K
- Magnetic pressure several orders of magnitude higher than plasma pressure ($\beta << 1$)
- Extends from the photosphere ($r_\odot$) to the base of the solar wind ($\sim 2r_\odot$)

# Relative Image Resolution

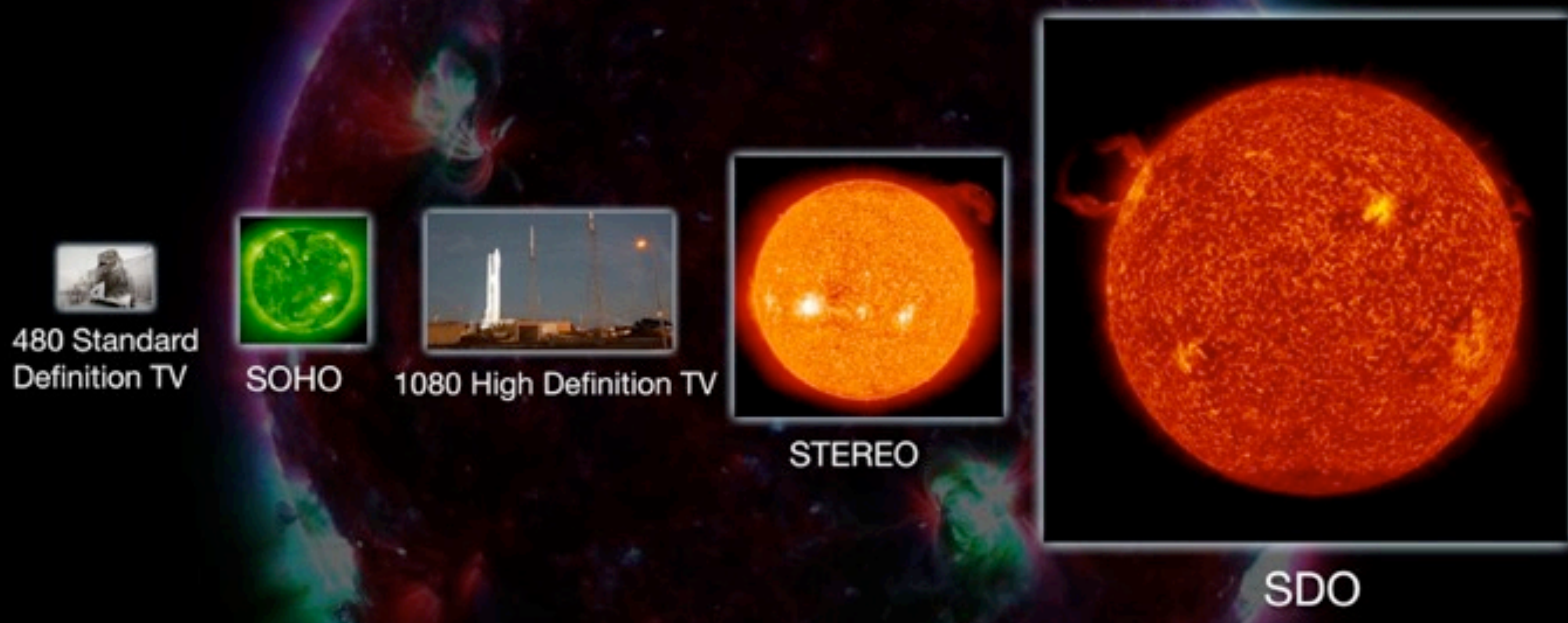

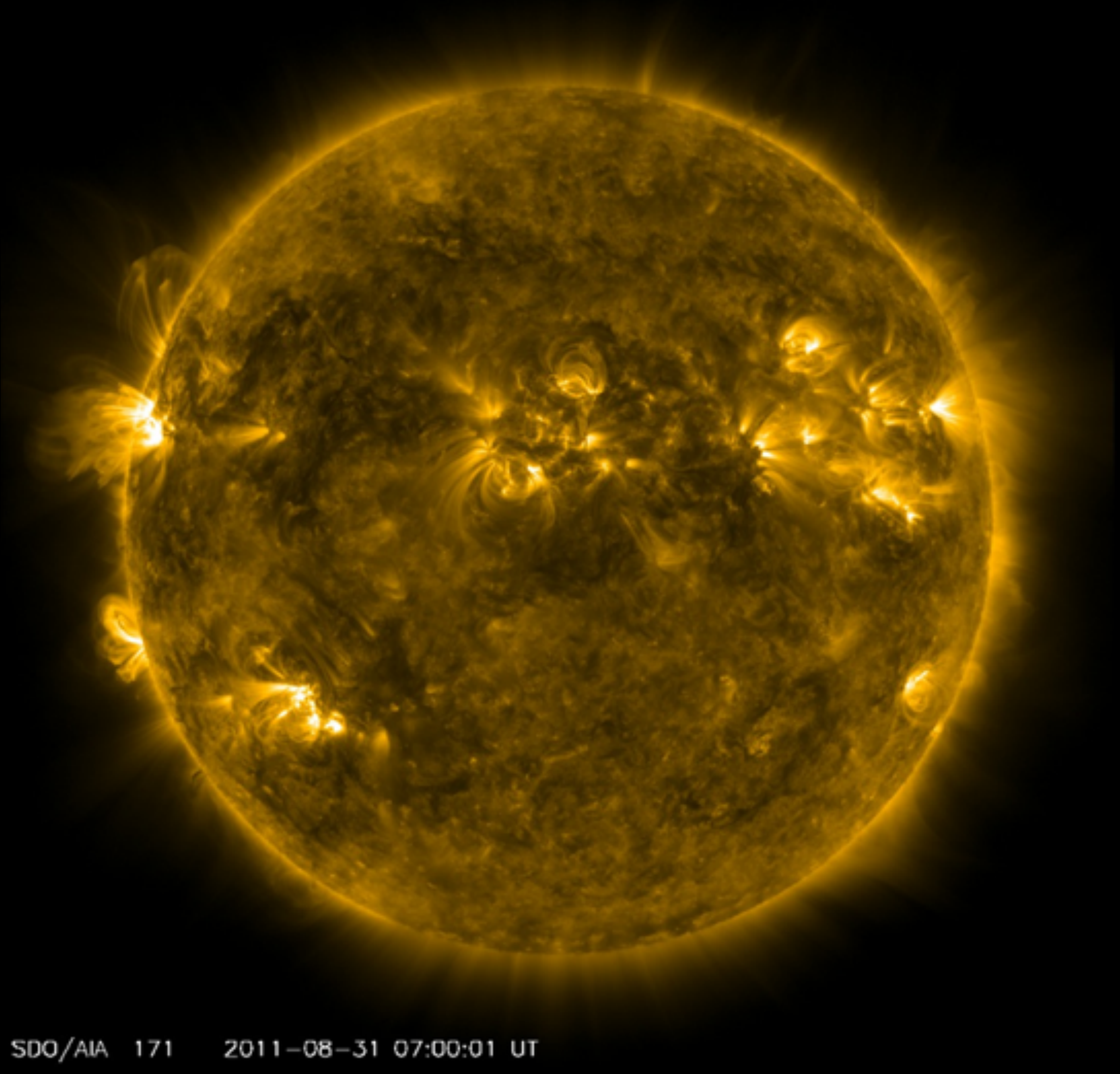
SDO/AIA 171 2011-08-31 07:00:01 UT

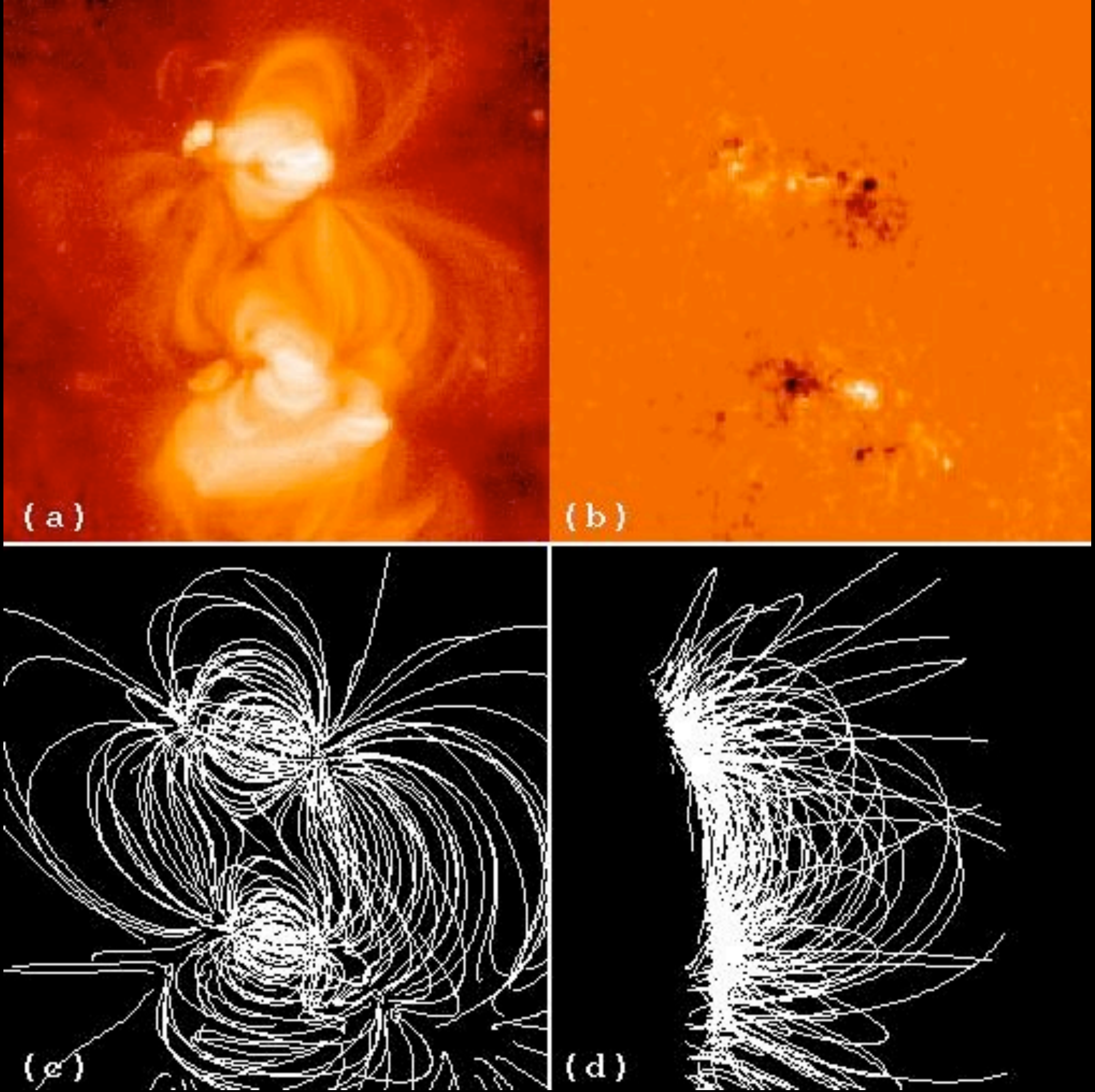
(a)
(b)
(c)
(d)

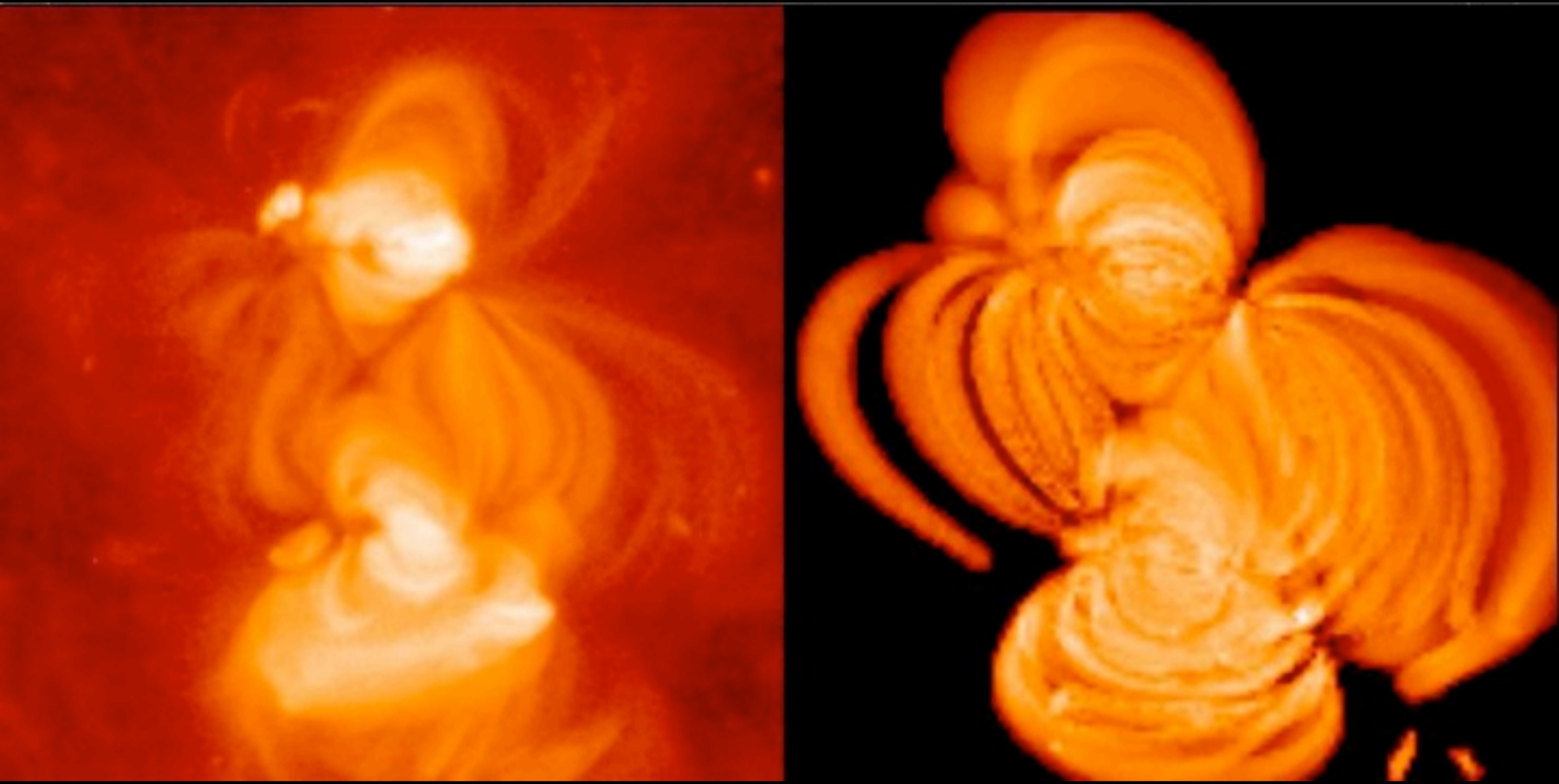

# NASA's STEREO Sees the Entire Sun

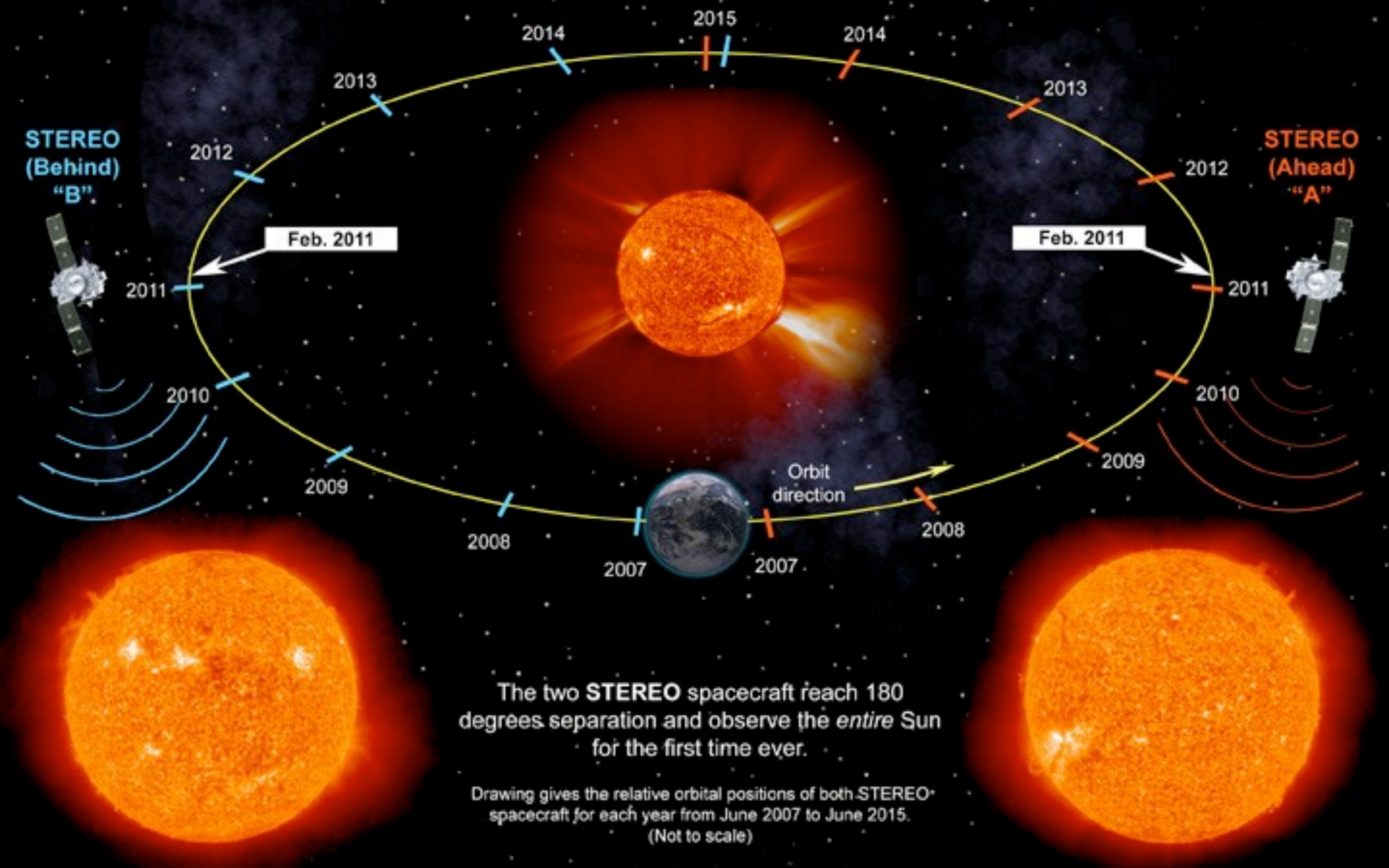


The two **STEREO** spacecraft reach 180 degrees separation and observe the *entire* Sun for the first time ever.

Drawing gives the relative orbital positions of both STEREO spacecraft for each year from June 2007 to June 2015.
(Not to scale)

# NUMERICAL METHODS

- Force-free magnetic fields satisfy the equations

$$(\nabla \times \mathbf{B}) \times \mathbf{B} = 0$$
$$\nabla \cdot \mathbf{B} = 0$$

- and the photospheric boundary condition

# NUMERICAL METHODS

- Force-free magnetic fields satisfy the equations

$$(\nabla \times \mathbf{B}) \times \mathbf{B} = 0$$
$$\nabla \cdot \mathbf{B} = 0$$

- and the photospheric boundary condition
- Potential: $\nabla \times \mathbf{B} = 0$

# NUMERICAL METHODS

- Force-free magnetic fields satisfy the equations

$$(\nabla \times \mathbf{B}) \times \mathbf{B} = 0$$
$$\nabla \cdot \mathbf{B} = 0$$

- and the photospheric boundary condition
- Potential: $\nabla \times \mathbf{B} = 0$
- Linear force-free: $\nabla \times \mathbf{B} = \alpha \mathbf{B}$

# NUMERICAL METHODS

- Force-free magnetic fields satisfy the equations

$$(\nabla \times \mathbf{B}) \times \mathbf{B} = 0$$
$$\nabla \cdot \mathbf{B} = 0$$

- and the photospheric boundary condition
- Potential: $\nabla \times \mathbf{B} = 0$
- Linear force-free: $\nabla \times \mathbf{B} = \alpha\mathbf{B}$
- Non-linear force-free

# NUMERICAL METHODS

- Direct extrapolation of boundary conditions: ill-posed problem for elliptic equations!
- Initial potential field, then progressively currents are introduced into the system: works for small deviations from potential field.
- MHD relaxation into force-free state: not too accurate.
- Optimization approach: requires vector magnetogram data at all boundaries of a computational box.
- Full MHD with solar wind.

# NUMERICAL METHODS

- Optimization approach:

Force-free magnetic fields have to obey the equations

$$(\nabla \times \mathbf{B}) \times \mathbf{B} = \mathbf{0}, \tag{1}$$

$$\nabla \cdot \mathbf{B} = 0. \tag{2}$$

We solve Equations (1) and (2) with the help of an optimization principle as proposed by Wheatland, Sturrock, and Roumeliotis (2000) and generalized by Wiegelmann (2004). Until now the method has been implemented in Cartesian geometry.

Here we define a functional in spherical geometry:

$$L = \int_V \left[B^{-2}\left|(\nabla \times \mathbf{B}) \times \mathbf{B}\right|^2 + |\nabla \cdot \mathbf{B}|^2\right] r^2 \sin\theta \, dr \, d\theta \, d\phi. \tag{3}$$

It is obvious that the force-free equations (1) and (2) are fulfilled when $L$ equals zero. We

# NUMERICAL METHODS

The force-free approach is valid in the low corona where the plasma $\beta$ is small. For extended structures, e.g., helmet streamers, the plasma $\beta$ increases and the force-free assumption is not valid anymore. Therefore it is necessary to consider the effect of plasma pressure and gravity here and solve the magneto hydrostatic equations (MHS)

$$\mathbf{j} \times \mathbf{B} - \nabla P - \rho \nabla \Psi = \mathbf{0}, \tag{4}$$

$$\nabla \times \mathbf{B} = \mu_0 \mathbf{j}, \tag{5}$$

$$\nabla \cdot \mathbf{B} = 0, \tag{6}$$

where $\mathbf{B}$ is the magnetic field, $\mathbf{j}$ the electric current density, $P$ the plasma pressure, $\rho$ the plasma density, $\mu_0$ the vacuum permeability and $\Psi$ the solar gravity potential. We define the functional

$$L = \int_V w(x, y, z)\ B^2\ (\Omega_a^2 + \Omega_b^2)\ \mathrm{d}^3x, \tag{7}$$

with

$$\mathbf{\Omega_a} = \begin{cases} B^{-2}\ [(\nabla \times \mathbf{B})] & \text{(force-free fields)}, \\ B^{-2}\ [(\nabla \times \mathbf{B}) \times \mathbf{B} - \mu_0(\nabla P + \rho \nabla \Psi)] & \text{(MHS)}, \end{cases} \tag{8}$$

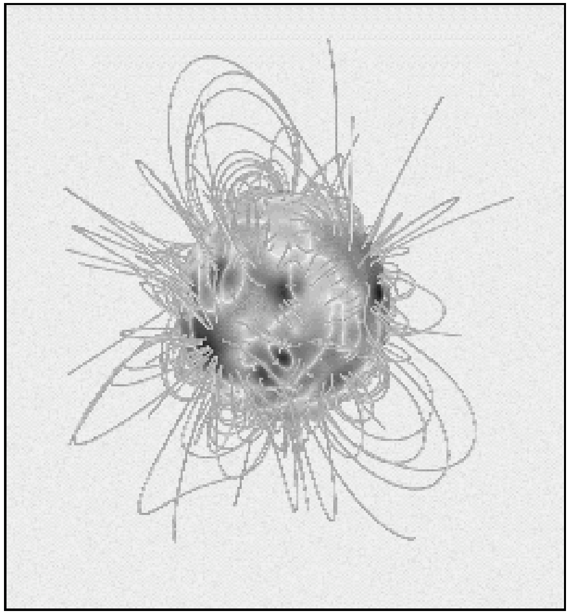
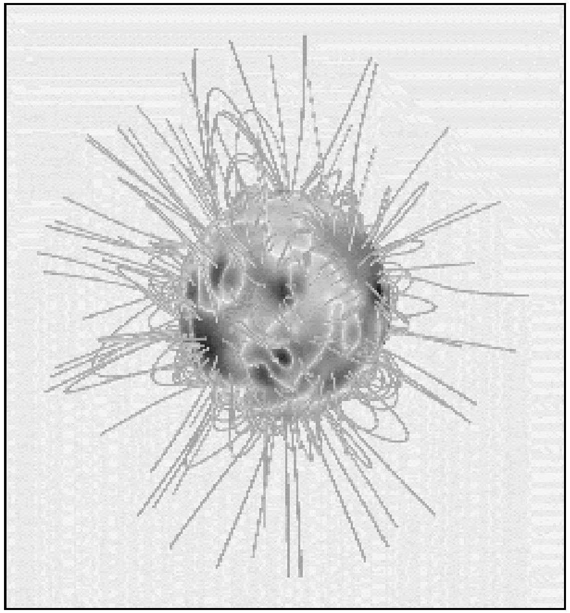
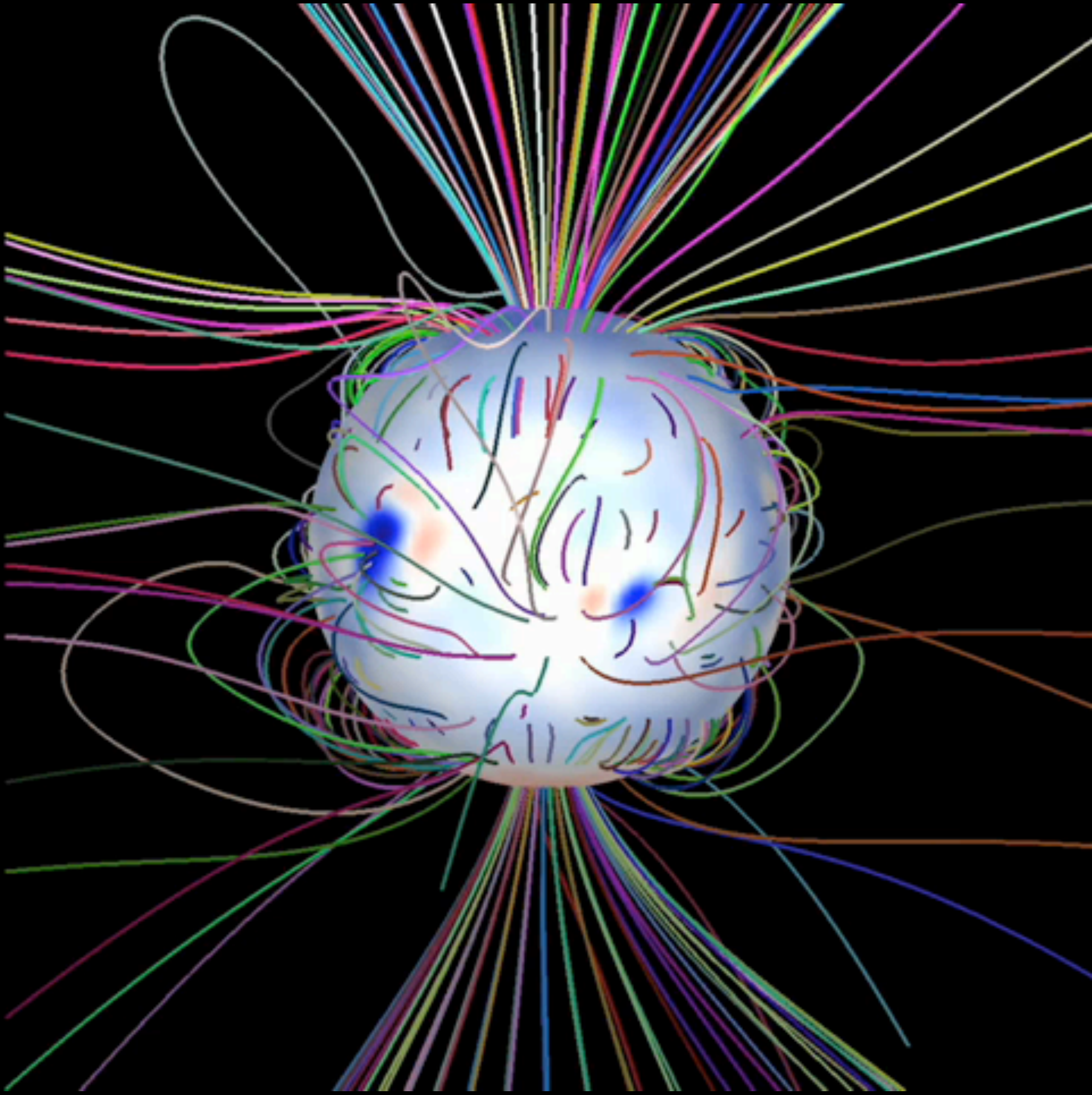

# NUMERICAL METHODS

- Full MHD with solar wind:

2.1. *Basic Equations*

The basic equations governing the simulated solar wind are the time-dependent MHD equations in the frame rotating with solar sidereal angular velocity $\boldsymbol{\Omega}$,

$$\frac{\partial \varrho}{\partial t} = -\nabla \cdot (\varrho \boldsymbol{V}), \tag{2}$$

$$\frac{\partial (\varrho \boldsymbol{V})}{\partial t} = -\nabla \left( P_g + \varrho \boldsymbol{V}\boldsymbol{V} - \frac{1}{4\pi}\boldsymbol{B}\boldsymbol{B} + \frac{B^2}{8\pi} \right) + \varrho [\boldsymbol{g} + (\boldsymbol{\Omega} \times \boldsymbol{r}) \times \boldsymbol{\Omega} + 2\boldsymbol{V} \times \boldsymbol{\Omega}], \tag{3}$$

$$\frac{\partial \boldsymbol{B}}{\partial t} = -\nabla (\boldsymbol{V}\boldsymbol{B} - \boldsymbol{B}\boldsymbol{V}), \tag{4}$$

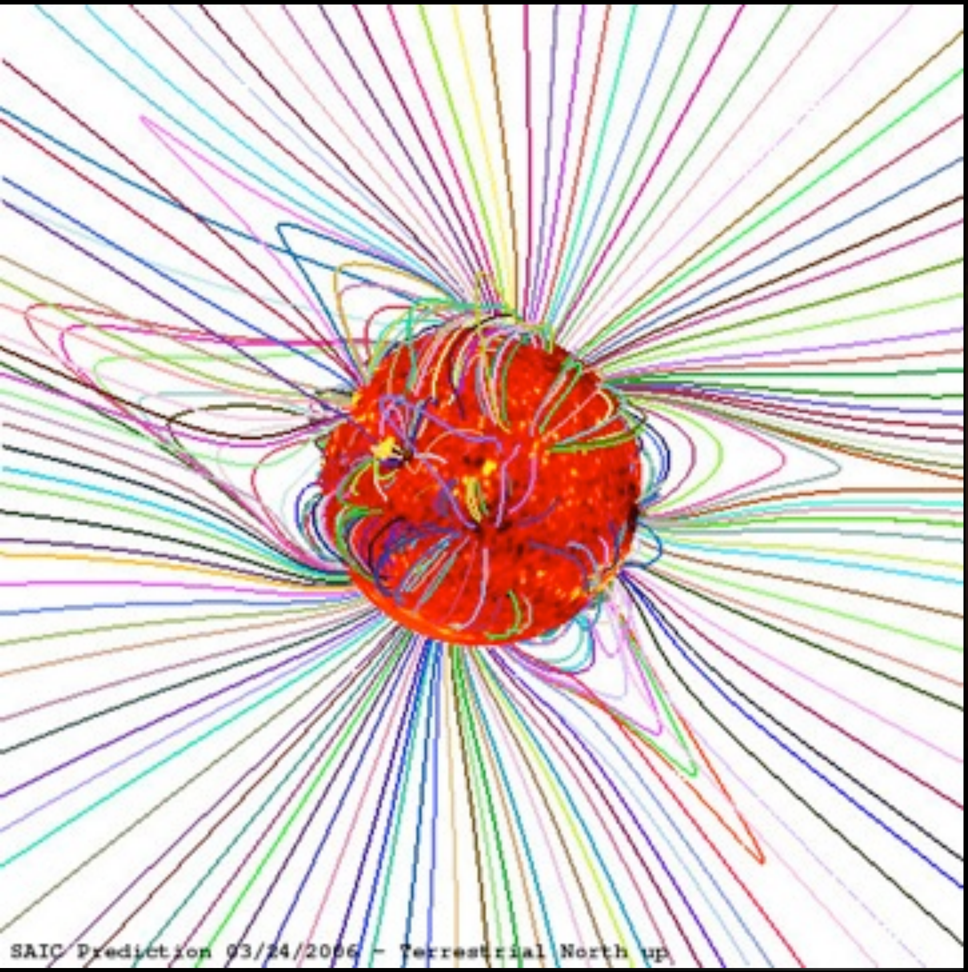


29/3/2006 Kastelorizo


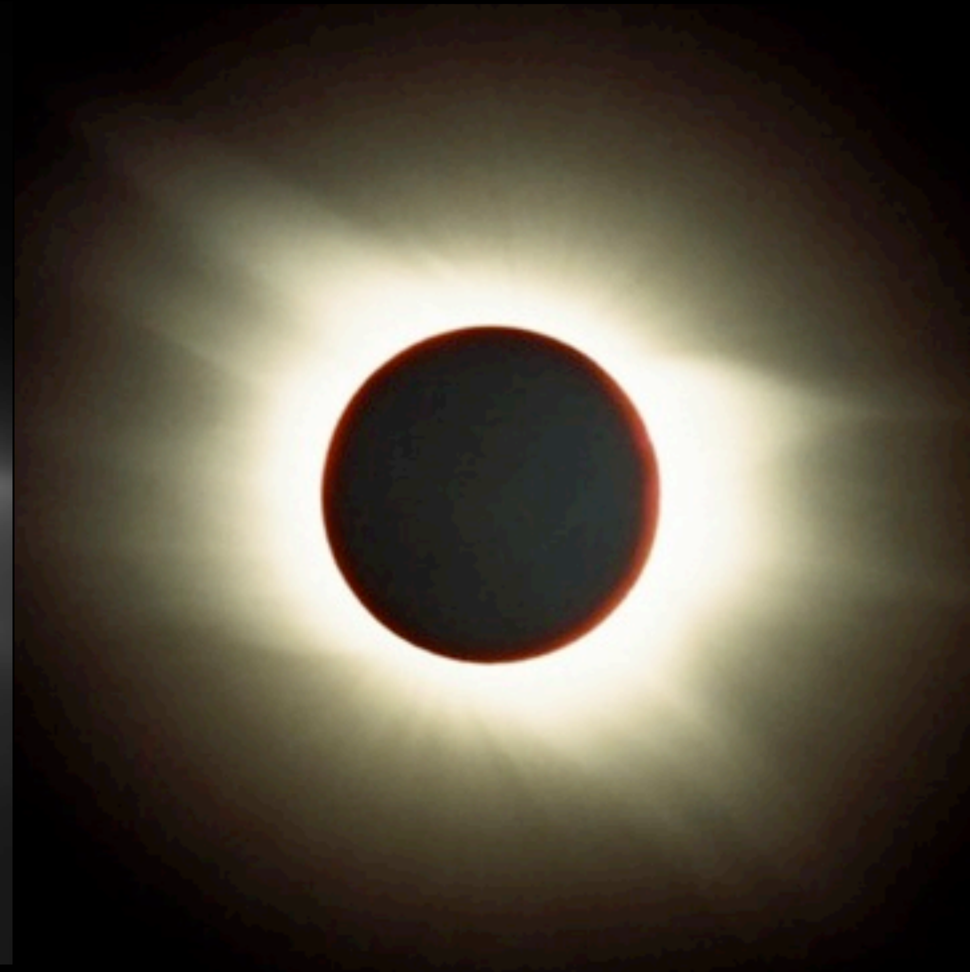

29/3/2006 Kastelorizo

# FORCE-FREE ELECTRODYNAMICS

Force-Free Electrodynamics (hereafter FFE) is a formal name for time-dependent electromagnetism in an ideal plasma with negligible inertia ($\rho = 0$) and negligible gas pressure ($\beta = 0$). The formalism of FFE has been developed for various relativistic astrophysical applications (pulsars, astrophysical jets, gamma-ray bursts, etc.) where the plasma supports electric currents and electric charges (Gruzinov, 1999). The equations of FFE are Maxwell's equations with nonzero electric fields as follows:

$$\frac{\partial \mathbf{E}}{\partial t} = c\nabla \times \mathbf{B} - 4\pi \mathbf{J} \ , \tag{1}$$

$$\frac{\partial \mathbf{B}}{\partial t} = -c\nabla \times \mathbf{E} \ , \tag{2}$$

$$\nabla \cdot \mathbf{B} = 0 \ . \tag{3}$$

These equations are coupled by the ideal MHD condition

$$\mathbf{E} \cdot \mathbf{B} = 0 \ , \tag{4}$$

implying that in an ideal plasma $\mathbf{E}$ and $\mathbf{B}$ are everywhere perpendicular, and the force-free condition

$$\rho_e \mathbf{E} + \frac{1}{c}\mathbf{J} \times \mathbf{B} = 0 \ . \tag{5}$$

Here, $\mathbf{J}$ is the electric current density, and $\rho_e \equiv (4\pi)^{-1}\nabla \cdot \mathbf{E}$ is the electric charge density. Gruzinov (1999) showed that it is possible to solve for $\mathbf{J}$ in the above set of equations and thus express the electric current density as a function of the electric and magnetic field, namely

$$\mathbf{J} = \frac{c}{4\pi}\nabla \cdot \mathbf{E} \ \frac{\mathbf{E} \times \mathbf{B}}{B^2} + \frac{c}{4\pi}\frac{(\mathbf{B} \cdot \nabla \times \mathbf{B} - \mathbf{E} \cdot \nabla \times \mathbf{E})}{B^2} \ \mathbf{B} \ . \tag{6}$$

One can then numerically integrate Maxwell's equations (eqs 1, 2) to obtain the time evolution of the electric and magnetic fields. We developed a three-dimensional (hereafter 3D) finite-difference time-domain (FDTD) cartesian FFE code with non-reflecting, perfectly absorbing outer boundaries applied successfully to the 3D structure of the pulsar magnetosphere (Kalapotharakos and Contopoulos, 2009; see also Yee, 1966; Spitkovsky, 2006).

Force-Free Electrodynamics (hereafter FFE) is a formal name for time-dependent electromagnetism in an ideal plasma with negligible inertia ($\rho = 0$) and negligible gas pressure ($\beta = 0$). The formalism of FFE has been developed for various relativistic astrophysical applications (pulsars, astrophysical jets, gamma-ray bursts, etc.) where the plasma supports electric currents and electric charges (Gruzinov, 1999). The equations of FFE are Maxwell's equations with nonzero electric fields as follows:

$$\frac{\partial \mathbf{E}}{\partial t} = c\nabla \times \mathbf{B} - 4\pi \mathbf{J} \ , \tag{1}$$

$$\frac{\partial \mathbf{B}}{\partial t} = -c\nabla \times \mathbf{E} \ , \tag{2}$$

$$\nabla \cdot \mathbf{B} = 0 \ . \tag{3}$$

These equations are coupled by the ideal MHD condition

$$\mathbf{E} \cdot \mathbf{B} = 0 \ , \tag{4}$$

implying that in an ideal plasma $\mathbf{E}$ and $\mathbf{B}$ are everywhere perpendicular, and the force-free condition

$$\rho_e \mathbf{E} + \frac{1}{c} \mathbf{J} \times \mathbf{B} = 0 \ . \tag{5}$$

Here, $\mathbf{J}$ is the electric current density, and $\rho_e \equiv (4\pi)^{-1} \nabla \cdot \mathbf{E}$ is the electric charge density. Gruzinov (1999) showed that it is possible to solve for $\mathbf{J}$ in the above set of equations and thus express the electric current density as a function of the electric and magnetic field, namely

$$\mathbf{J} = \frac{c}{4\pi} \nabla \cdot \mathbf{E} \, \frac{\mathbf{E} \times \mathbf{B}}{B^2} + \frac{c}{4\pi} \frac{(\mathbf{B} \cdot \nabla \times \mathbf{B} - \mathbf{E} \cdot \nabla \times \mathbf{E})}{B^2} \mathbf{B} \ . \tag{6}$$

One can then numerically integrate Maxwell's equations (eqs 1, 2) to obtain the time evolution of the electric and magnetic fields. We developed a three-dimensional (hereafter 3D) finite-difference time-domain (FDTD) cartesian FFE code with non-reflecting, perfectly absorbing outer boundaries applied successfully to the 3D structure of the pulsar magnetosphere (Kalapotharakos and Contopoulos, 2009; see also Yee, 1966; Spitkovsky, 2006).

# FORCE-FREE ELECTRODYNAMICS

- When electric fields die out:

$$\mathbf{J} = \frac{c}{4\pi}\nabla \times \mathbf{B}$$

$$\nabla \cdot \mathbf{B} = 0$$

$$\mathbf{J} \times \mathbf{B} = 0$$

- The final FFE equilibrium solution can be viewed as a solution of the above equations satisfying a given normal-field distribution on the boundary.
- Given the ill-posed nature of this problem (only the normal field component on the boundary is known), this solution is not unique and depends on the initial magnetostatic configuration and on the course toward equilibrium.

# FORCE-FREE ELECTRODYNAMICS

- Time relaxation:

*i*) Start with a simple static potential magnetic field distribution such as $\mathbf{B} = 0$ everywhere, or a dipolar field of any direction, etc.

*ii*) Evolve the vertical photospheric magnetic field by imposing a distribution of horizontal photospheric electric fields using Faraday's equation (eq. 2). This distribution is chosen such that the resulting photospheric magnetic field asymptotically ($t \to \infty$) approaches a given photospheric magnetogram (see next section).

*iii*) During the evolution of the photospheric magnetic field, force-free electrodynamic waves are injected from the photosphere into the corona. Assuming non-reflecting, perfectly absorbing conditions at large distances, these waves will be absorbed by the outer boundaries and will not re-enter the computational domain. The moving electric charges carried by these waves begin to establish a nonlinear network of coronal electric currents.

*iv*) Gradually, as the photospheric magnetic field distribution approaches the target, photospheric electric fields will correspondingly decrease, and as a consequence magnetospheric electrodynamic waves, electric fields, and electric charges will also asymptotically fade. The nonlinear network of coronal electric currents, however, will survive.

*v*) When electric fields vanish everywhere, we relax to a force-free configuration that closely matches the given photospheric boundary condition.

At $t = 0$, we populate our 2D grid with a particular force-free magnetostatic field configuration $B_z(i,j;t=0)$ that can be anything (i.e., zero, dipole-like of any direction and strength, quadrupole-like, etc.). Our aim is to impose a particular horizontal electric field distribution that will asymptotically evolve $B_z$ toward a target magnetic field configuration $B_T(i,j)$. We chose the following procedure: given the photospheric magnetic field distribution $B_z(i,j;t)$ at each time step $t$, we scan the full photospheric grid $(i,j)$, and at each cell position we add four electric field components at the four edges of the cell such that

$$\begin{aligned}
E_x(i,j;t) &\rightarrow E_x(i,j;t) - f[B_T(i,j) - B_z(i,j;t)] \ , \\
E_y(i,j;t) &\rightarrow E_y(i,j;t) + f[B_T(i,j) - B_z(i,j;t)] \ , \\
E_x(i,j+1;t) &\rightarrow E_x(i,j+1;t) + f[B_T(i,j) - B_z(i,j;t)] \ , \\
E_y(i+1,j;t) &\rightarrow E_y(i+1,j;t) - f[B_T(i,j) - B_z(i,j;t)] \ ,
\end{aligned} \tag{10}$$

as shown in Fig. 1a. Here $f$ is a free positive numerical factor used to adjust the rate of convergence. We chose $f = 0.5$, as convergence becomes numerically unstable for $f > 0.5$ and too slow for $f < 0.5$. At each time step $t$, we start with $E_x(i,j;t) = E_y(i,j;t) = 0$ everywhere, and then scan the 2D grid and update electric fields according to eqs. (10). In the first cell where the algorithm is applied, Faraday's equation (eq. 2) can be written in a first-order discretized form as follows:

$$\frac{\partial B_z(i,j;t)}{\partial t} = \frac{4cf[B_T(i,j) - B_z(i,j;t)]}{\delta} \ . \tag{11}$$

If we only had one computational grid-cell, this equation would be integrated numerically to obtain the asymptotic solution $B_z(i,j;t \rightarrow \infty) = B_T(i,j)$. When the algorithm is applied sequentially to the full horizontal grid, electric fields on edges that correspond to neighboring cells will be updated twice as the algorithm is applied in both cells. In the sketch of Fig. 1b-f, one can see how the electric

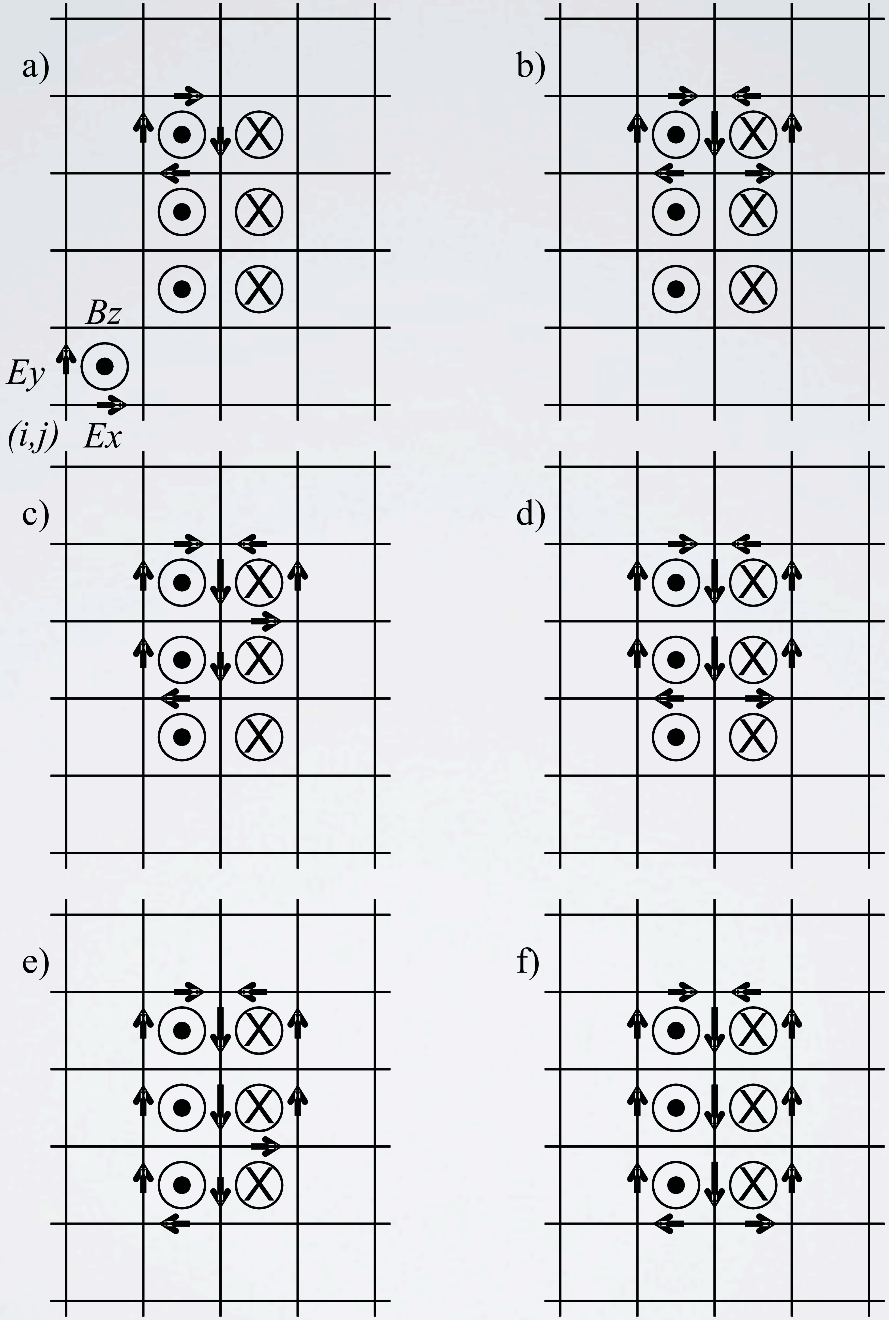
a)
b)
c)
d)
e)
f)
Bz
Ey
(i,j)
Ex

# RESULTS

- Numerical runs:
  - Cartesian staggered grid (resolution: $2^o \times 2^o$ or $25 \times 25$ $Mm^2$)
  - Integration method: FDTD, 3rd order Runge-Kutta
  - Perfectly absorbing non-reflecting outer boundary (PML)
  - Duration: 24 hours for 10,000 time integration steps
- Test case: `Halloween 2003' period

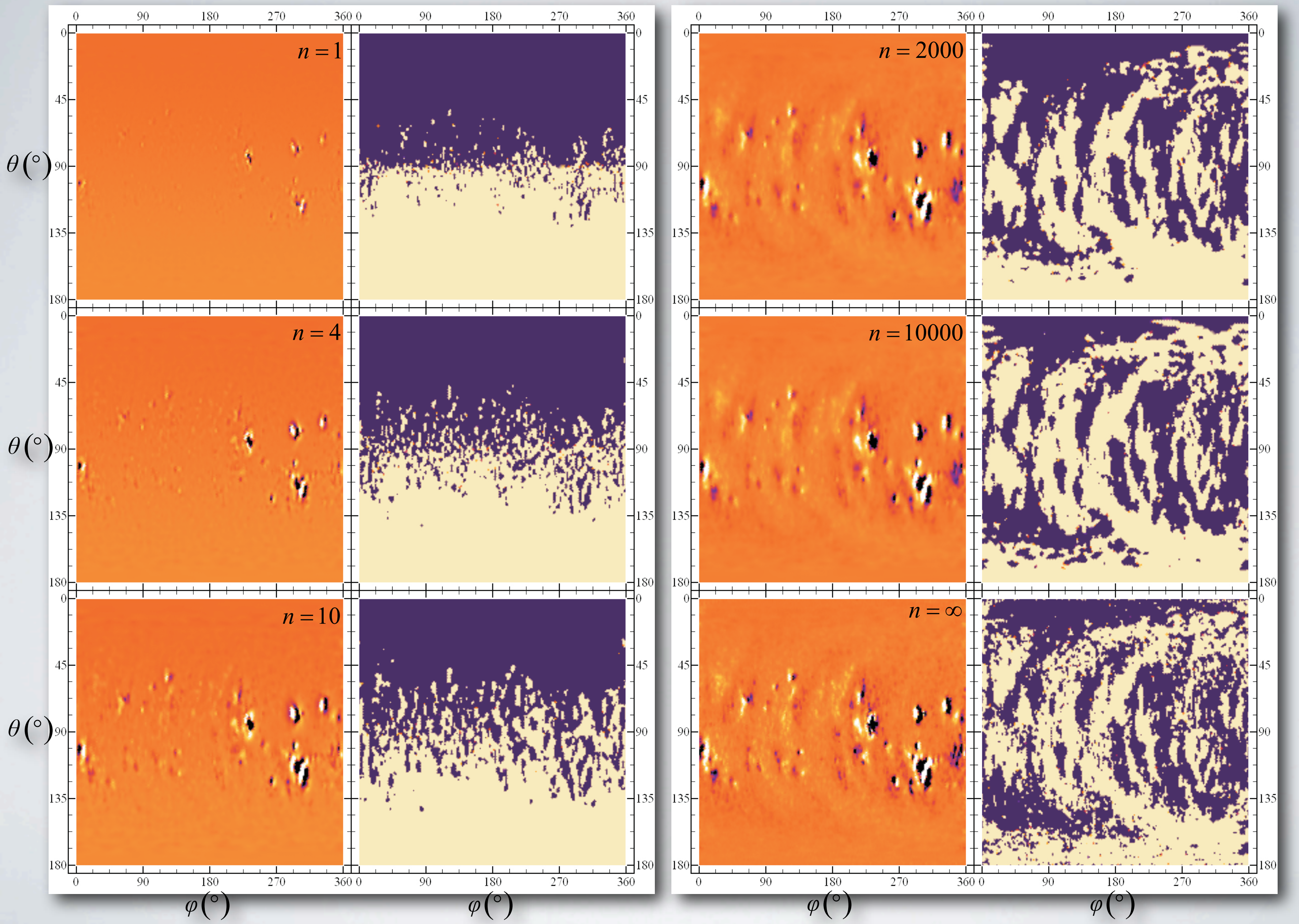

n = 1
n = 4
n = 10
n = 2000
n = 10000
n = ∞
θ (°)
φ (°)
0
45
90
135
180
0
90
180
270
360

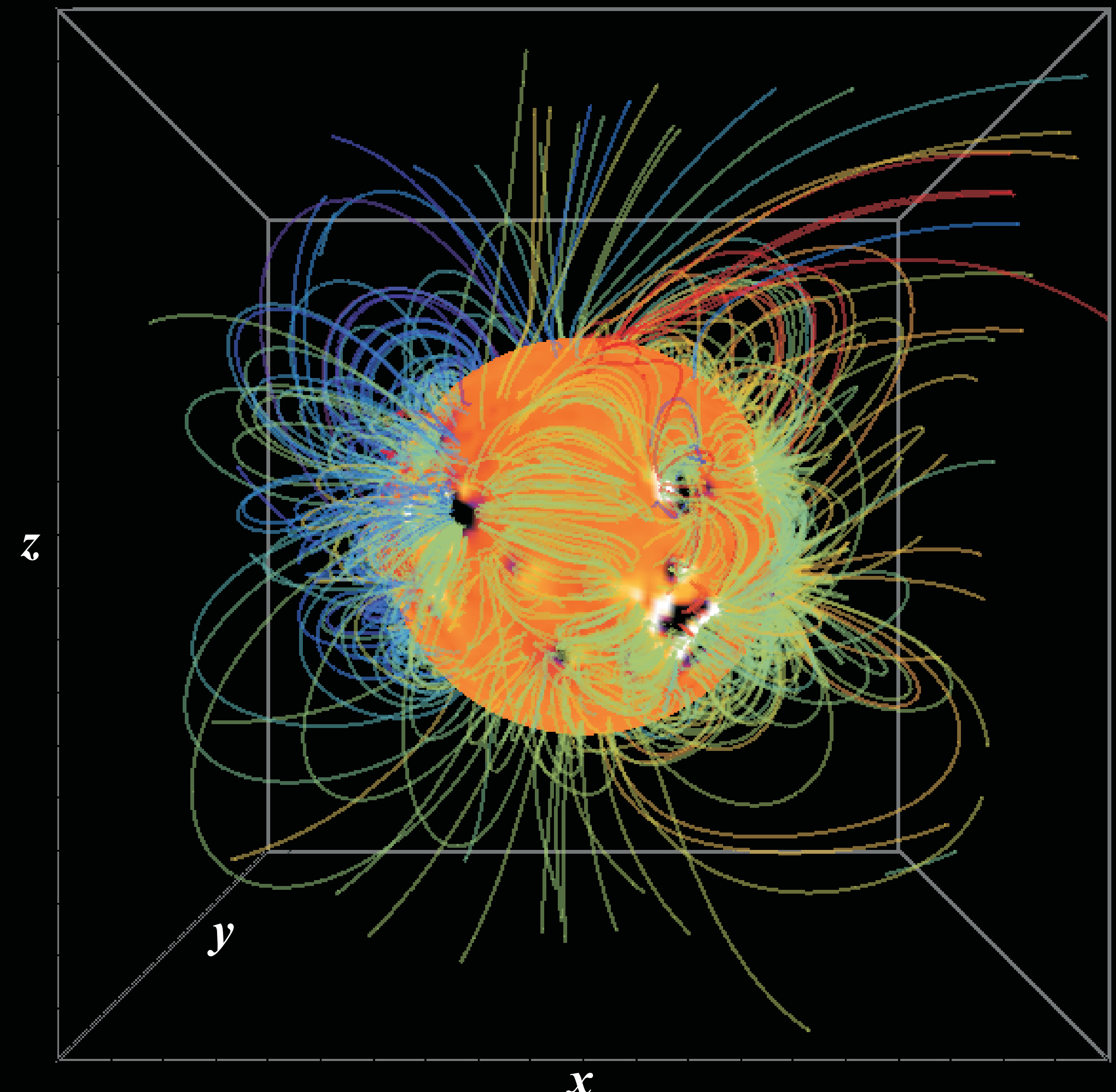

z
y
x

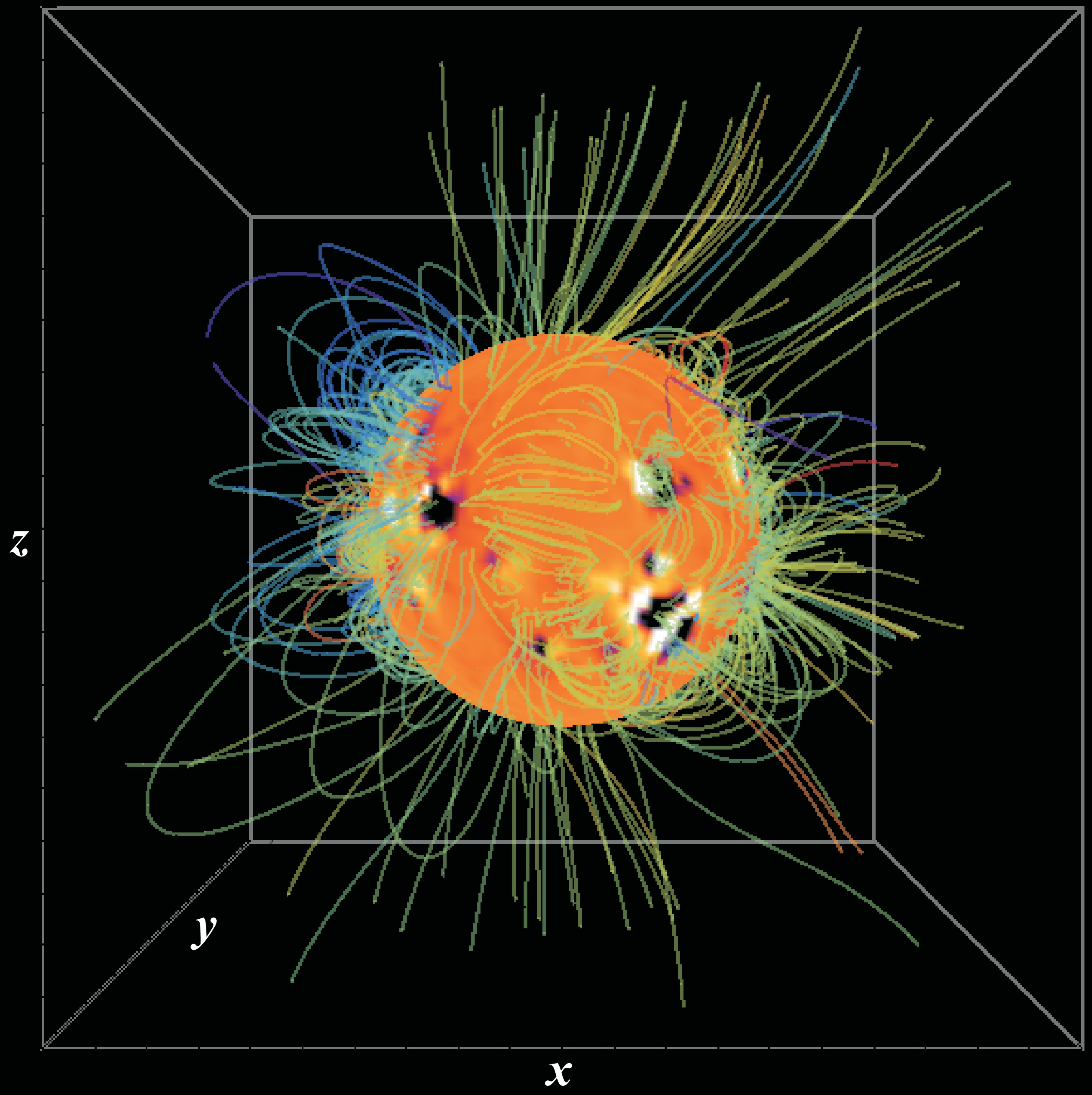
z
y
x

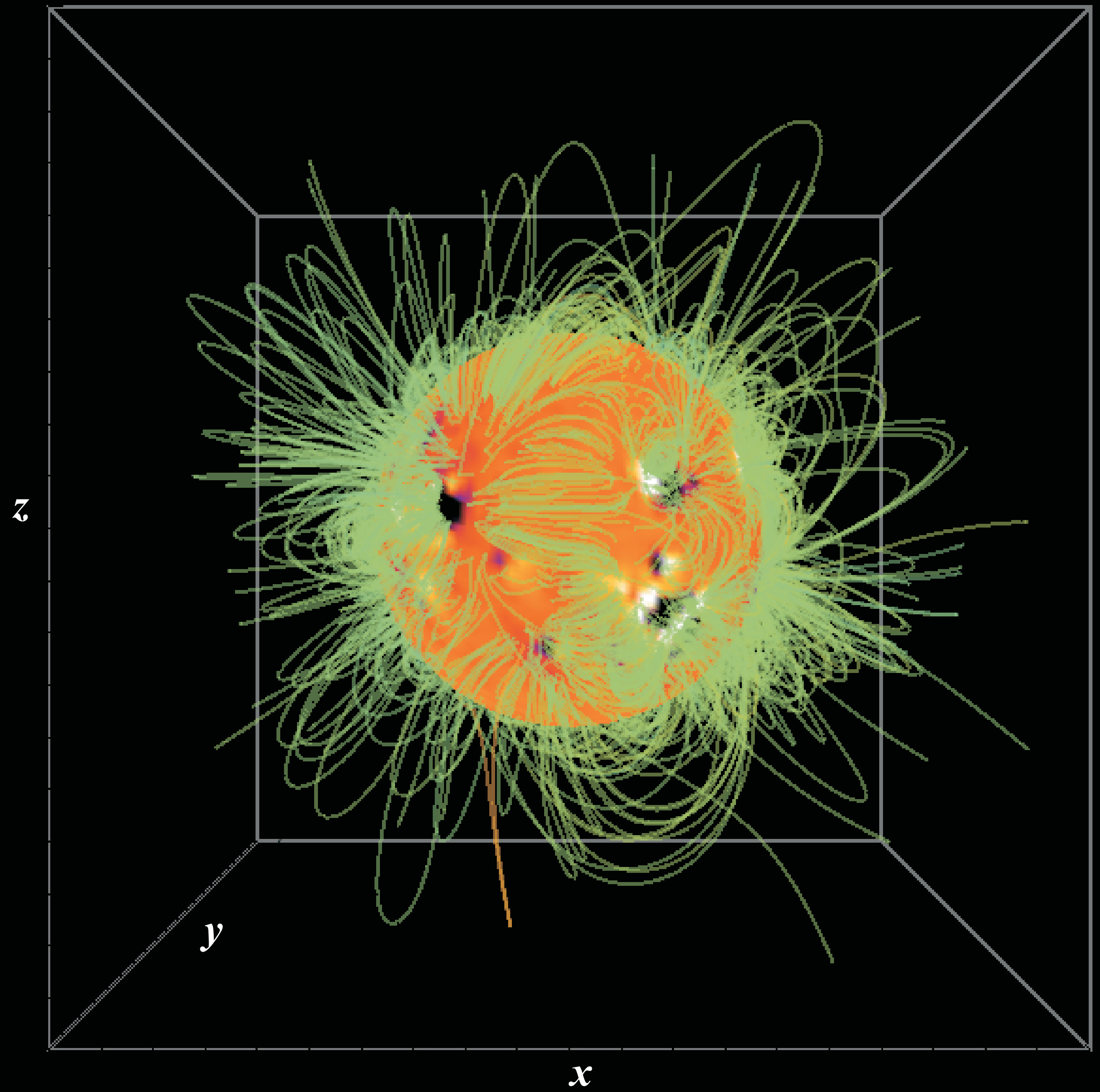
z
y
x

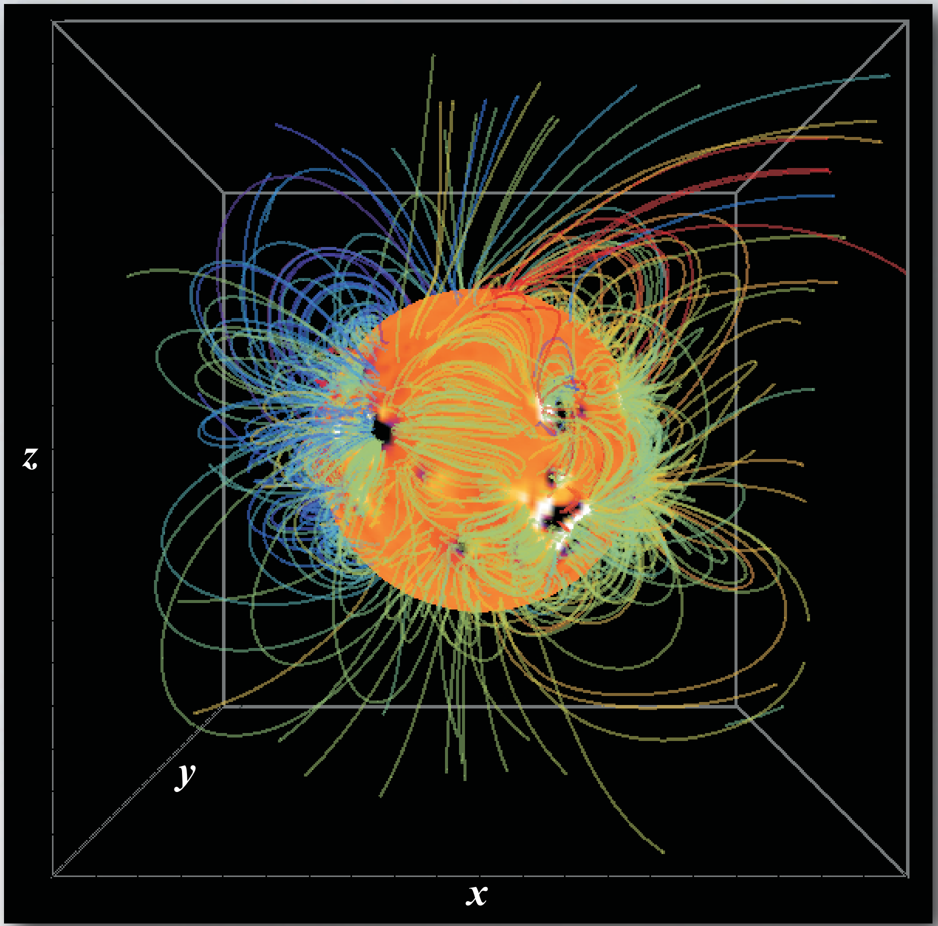
z
y
x

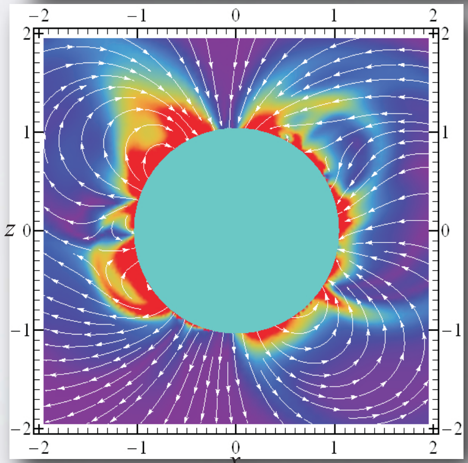
−2 −1 0 1 2
z
x

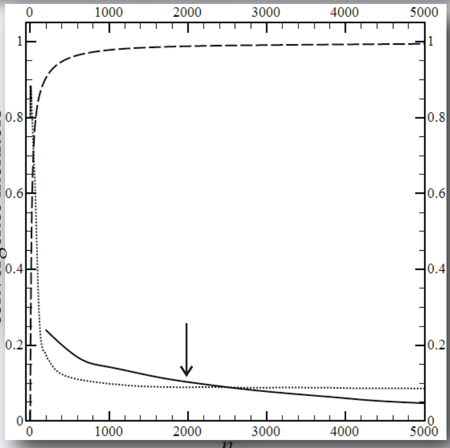
0 1000 2000 3000 4000 5000
0 0.2 0.4 0.6 0.8 1
convergence monitors
n

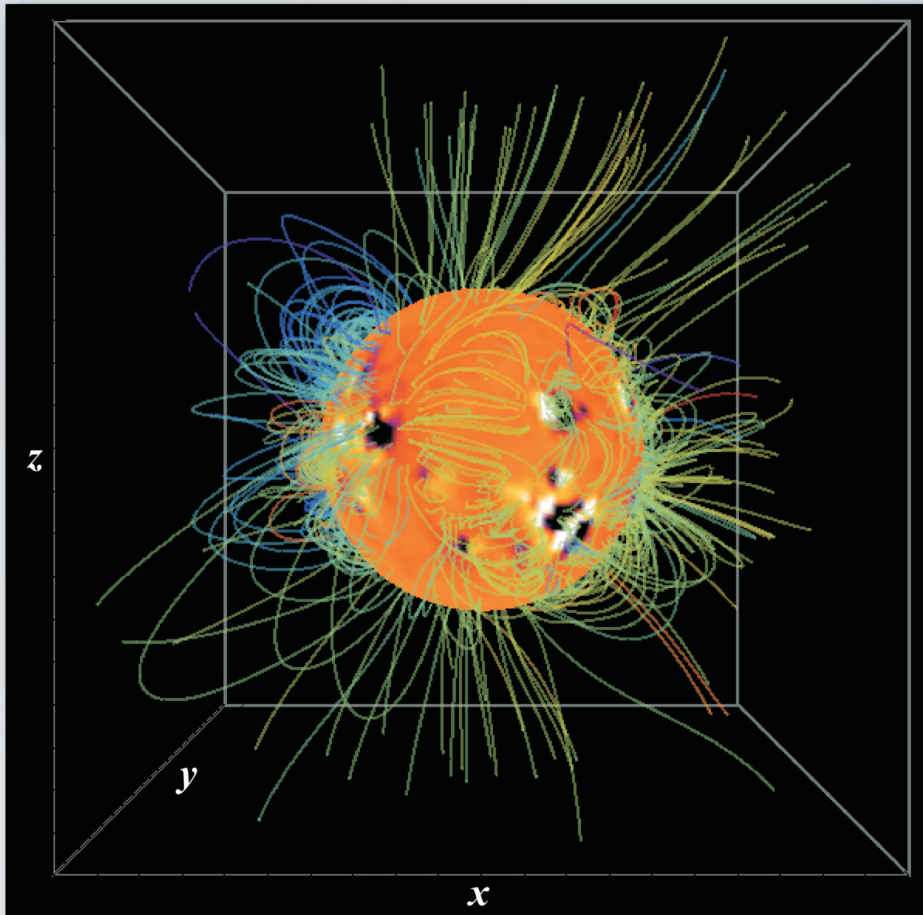

z
y
x


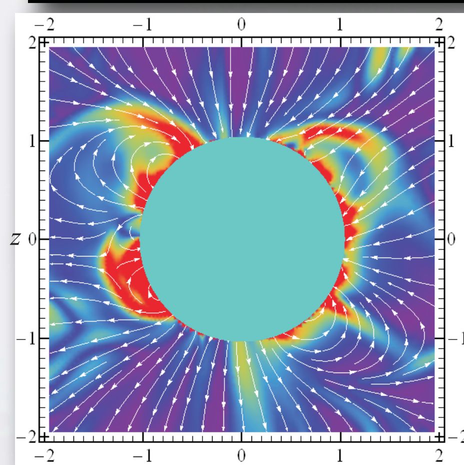

−2 −1 0 1 2
z
x


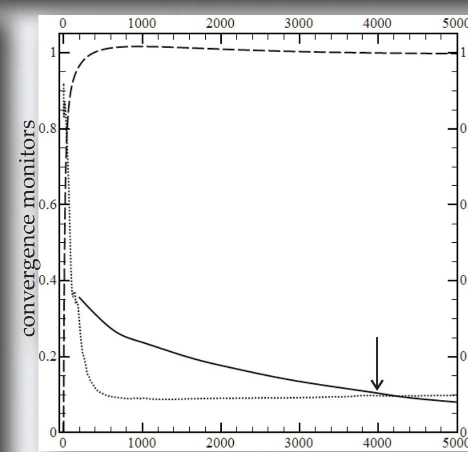

0 1000 2000 3000 4000 5000
0 0.2 0.4 0.6 0.8 1
convergence monitors
n

# PROSPECTS FOR THE FUTURE

- Study localized active regions:

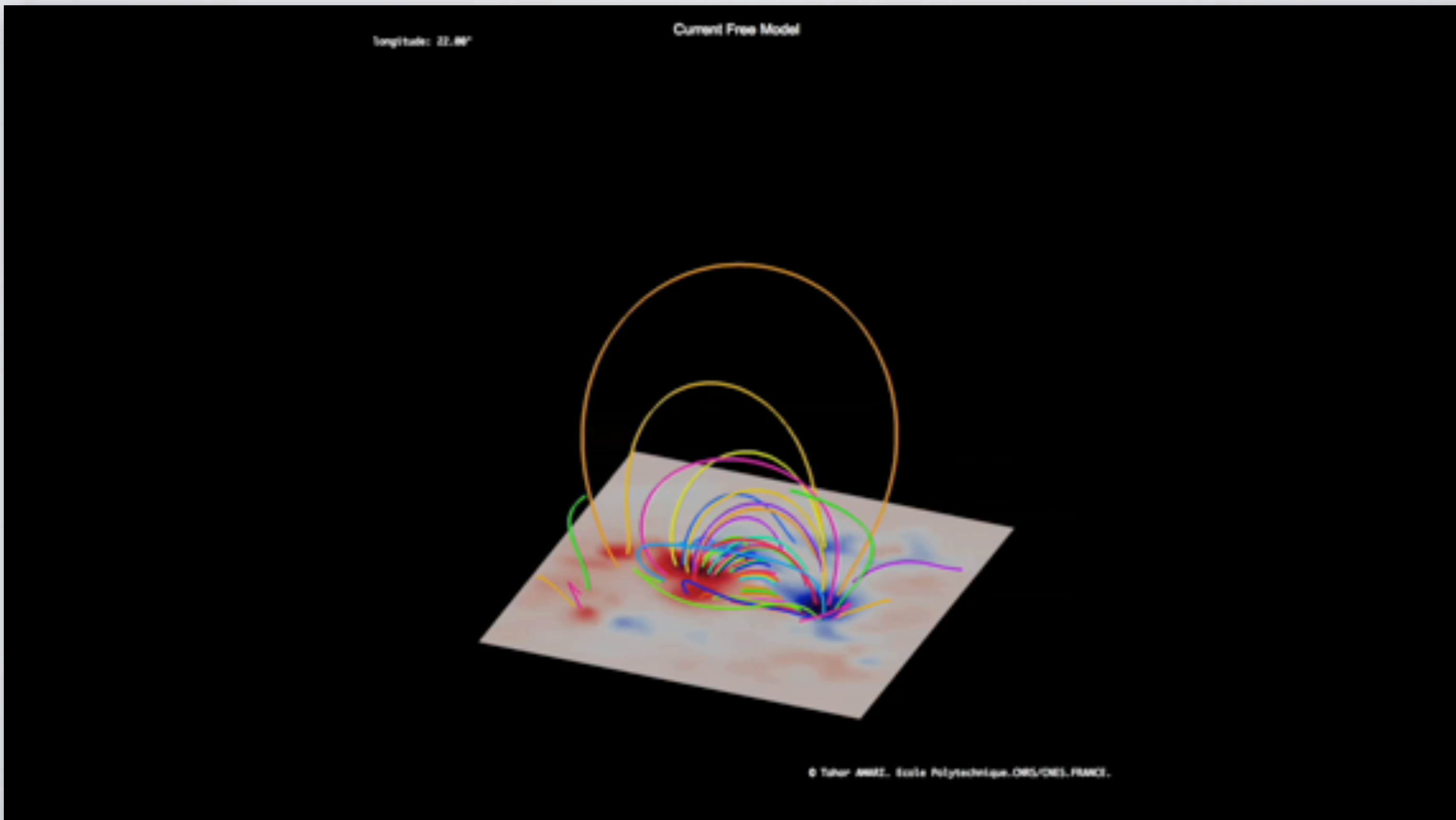

# PROSPECTS FOR THE FUTURE

- Space weather prediction (?)

End of Cycle 23
(solar minimum)

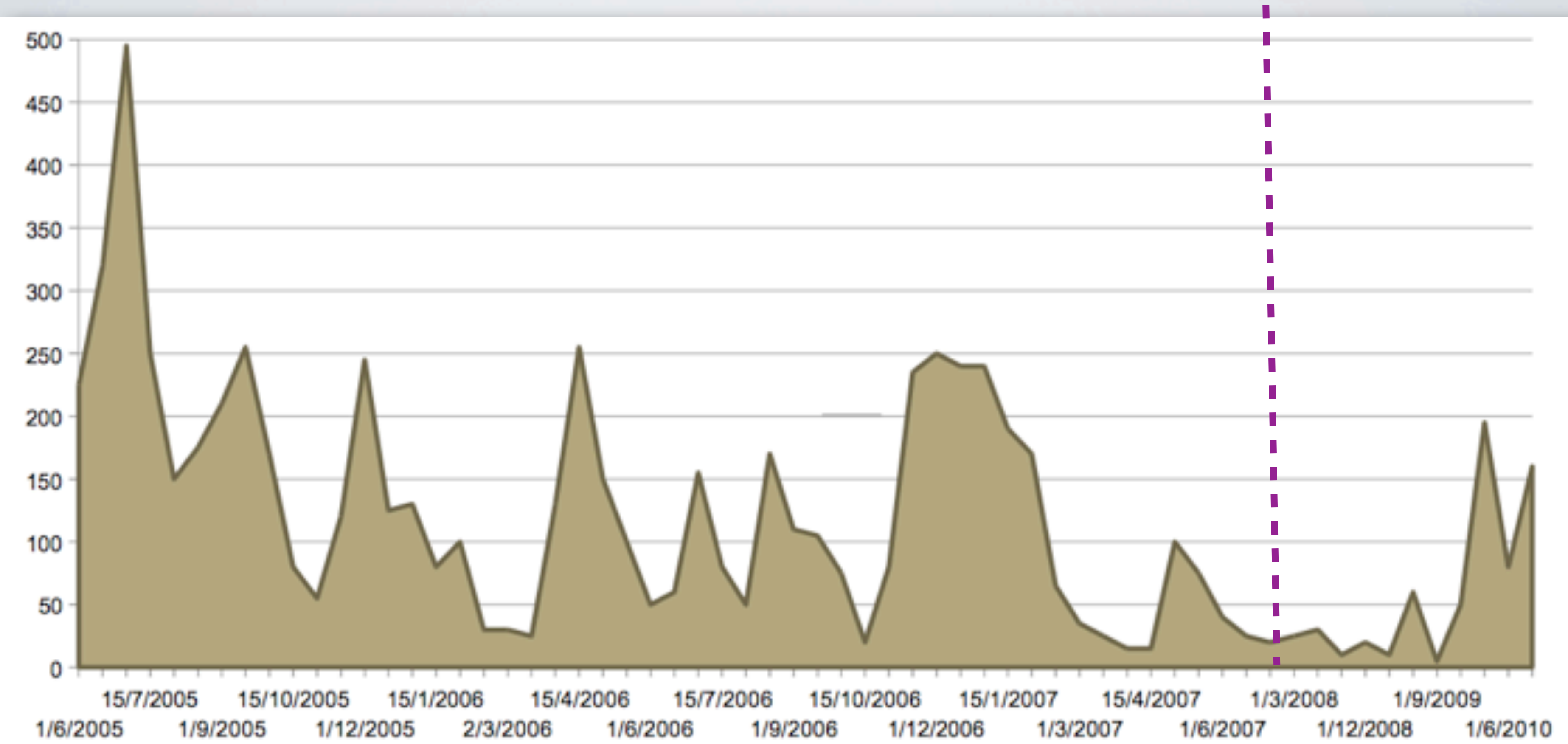


Evolution of Magnetic Field Energy

# PROSPECTS FOR THE FUTURE

- Space weather prediction (?)

End of Cycle 23
(solar minimum)

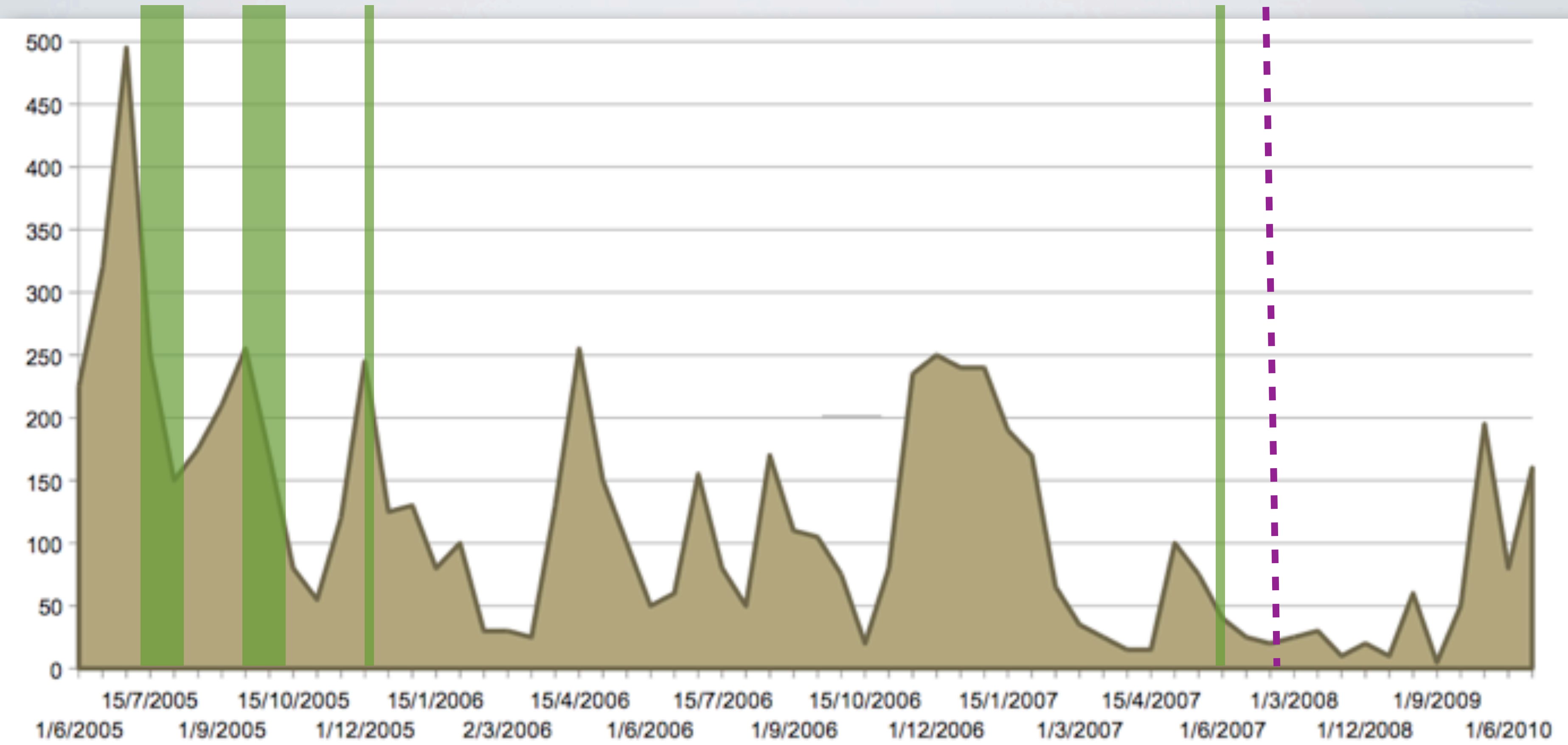


Evolution of Magnetic Field Energy

# PROSPECTS FOR THE FUTURE

- Space weather prediction (?)

End of Cycle 23
(solar minimum)

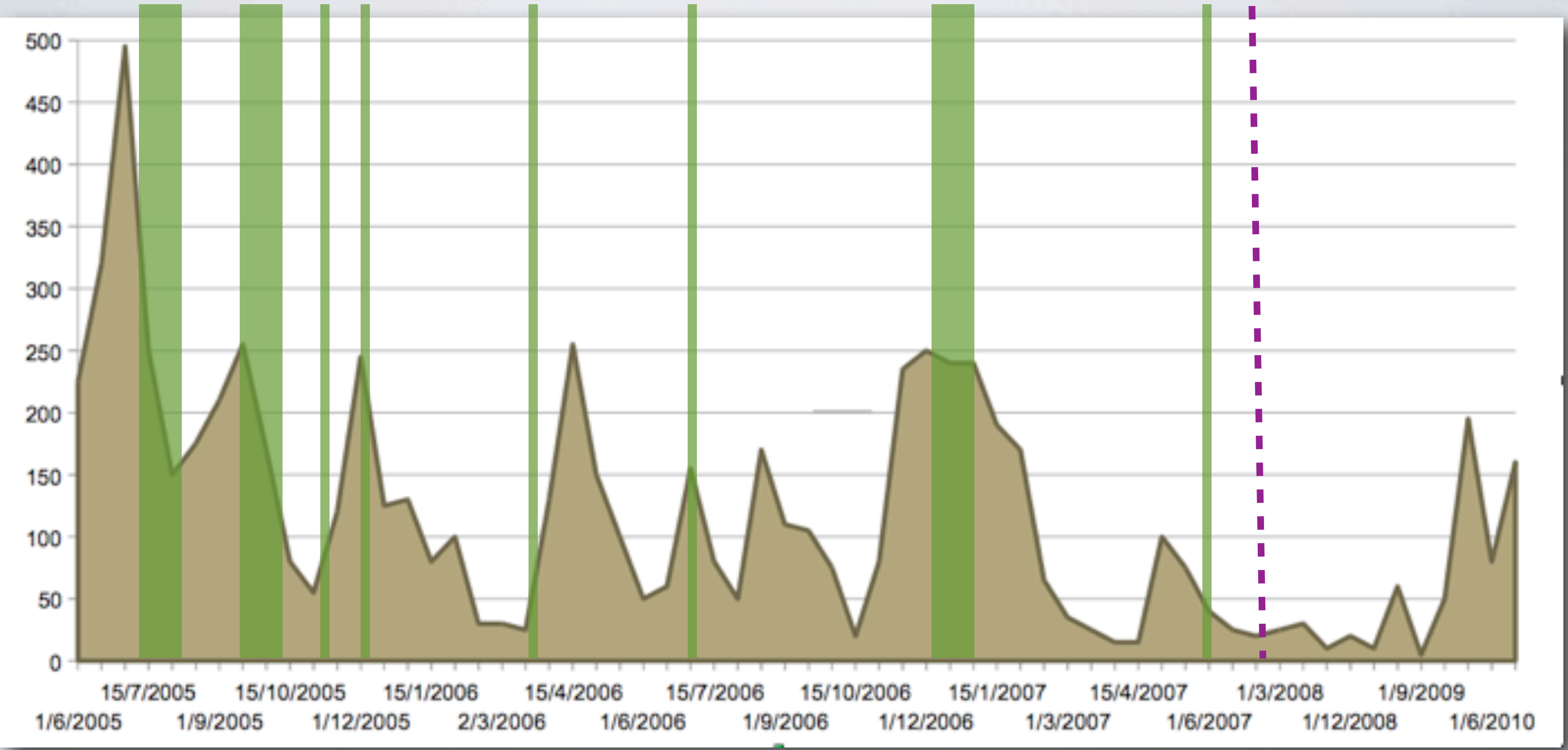


Evolution of Magnetic Field Energy

# PROSPECTS FOR THE FUTURE

- Space weather prediction (?)

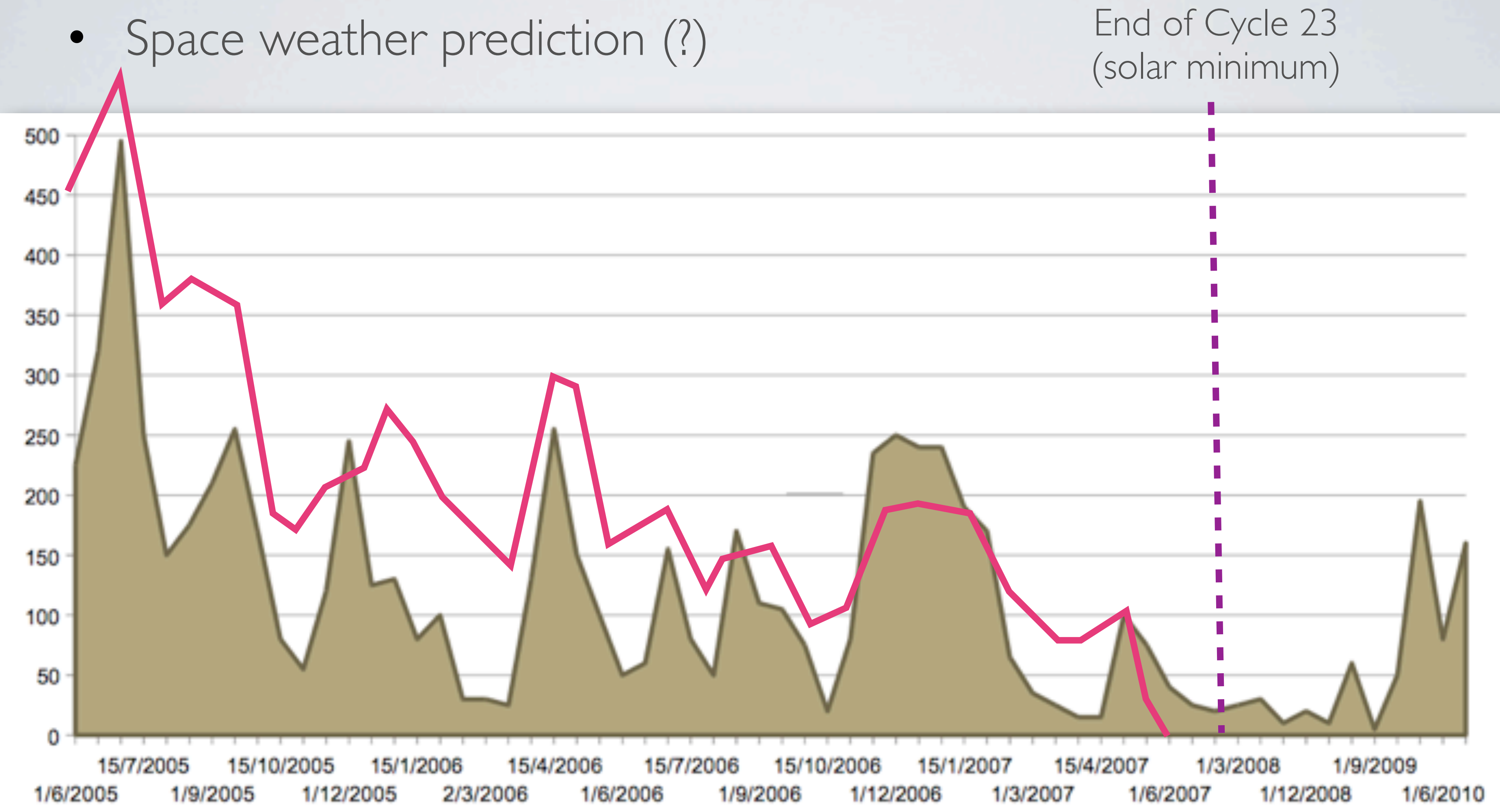


Evolution of Magnetic Field Energy

# PROSPECTS FOR THE FUTURE

- Magnetic Helicity:

$$\mathcal{H} = \int_V \mathbf{A} \cdot \mathbf{B} \, \mathrm{d}V$$

$$\frac{\partial \mathbf{B}}{\partial t} = -c\nabla \times \mathbf{E}$$

$$\mathbf{B} = \nabla \times \mathbf{A}$$

$$\frac{\partial \mathbf{A}}{\partial t} = -c\mathbf{E}$$

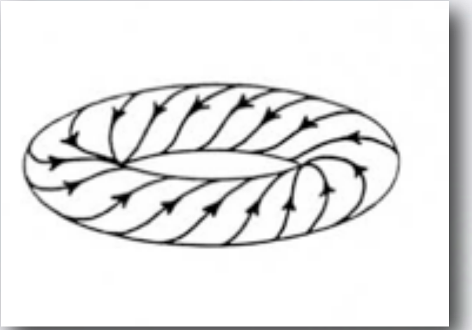

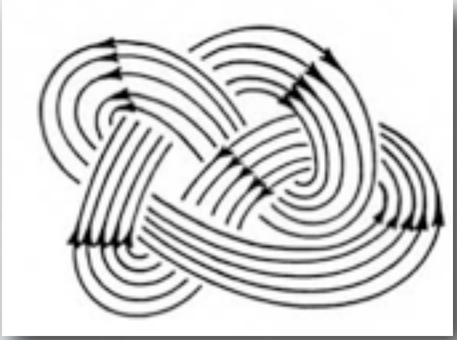

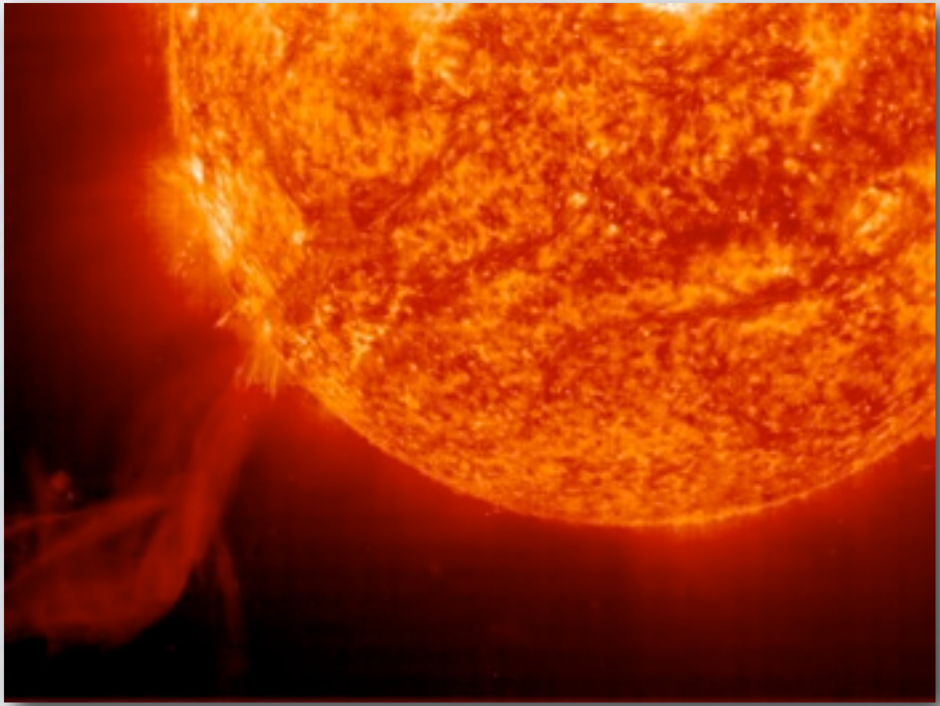

# PROSPECTS FOR THE FUTURE

- Numerical code improvements:
    - Rigorous testing
    - Proper LOS MF deprojection
    - Spherical coordinates
    - Outer boundary conditions: radial MF
    - Parallelization (MPI)
    - Visualization